CHAPTER-5

A Flexible Low-Voltage Operated Ammonia Sensor based on Polymer/2D g-C3N4 Nanocomposite and Hybrid Dielectric (ZrOx/PMMA/PMCF) Film

The part of the work is adopted from-

A. Verma, S. Gupta, V. N. Mishra, and R. Prakash, "**A Low-Voltage, Self-Oriented Organic Polymer Nanocomposite-Based Flexible TFT for Ammonia Gas Sensing at Room Temperature**," ***IEEE Transactions on Electron Devices*****,** vol. 70, no. 5, pp. 2453-2459, May 2023, ***doi: 10.1109/TED.2023.3255835.***

Abstract— The current study includes the fabrication and characterization of a novel, low-voltage, flexible organic thin film transistor (OTFT) for ammonia sensing at room temperature (RT 25 ºC). The device fabrication process uses a hybrid (inorganic oxide/polymer) dielectric layer as a gate oxide and a polymer/2D nanocomposite as an active layer. The UV-cured synthesized hybrid dielectric layer of ZrOx/PMMA/PMCF passes with a very smooth film (RMS roughness-0.388 nm) (thickness -55±4 nm), the high areal capacitance of 310 nF/cm^2, dielectric constant of ~20, low leakage current density of ~10^{-9} A/cm^2 at -2 V, and a high band gap of 5.27 eV. A uniform thickness of 35±4 nm polymer nanocomposite layer, deposited by the solution-casted floating film transfer (FTM) technique, has been used to investigate the electrical characteristics of the flexible sensor in terms of I/V plot, subthreshold swing, mobility, etc. The bending test of the device has been performed over the curved holder and shows a reliable performance with solution-processed hybrid dielectric and polymer nanocomposite film. Using polymer/2D nanocomposite material as a sensing layer offers a low detection of 500 ppb, a sensing response of 69%, and a fast response/recovery time of 4±0.5/36±4 sec. over 20 ppm ammonia gas. The fabricated flexible device, therefore, has a potential application in the area of low voltage operated OTFT for ammonia sensing application.

5.1 Introduction

organic semiconductor-based thin film transistor has gained more interest due to two major applications: (a) flexible electronics, such as flexible LEDs, displays, keyboards, smartphones, sensors, memories, etc., [202][203] (b) flexible smart cards, such as RFID (Radio frequency identification tags, etc. [203]. The flexible, low-temperature processing, large

area coverage and cost -efficient properties of the organic semiconductors made them viable choice for broad area flexible electronic and sensing applications. A good flexible electronic device must maintain its satisfactory performance when subject to folding, mechanical bending, expansion, and compression [202]. To fulfill the above criteria, the fabrication processes on the flexible substrates must be carefully investigated, such as substrate handling, low-temperature processing, film adhesion issues, etc. For example, the twisted/curled or, when heated, handled with a tweezer results in a non-uniform deposition, cracks, defects, etc. [203][204]. The choice of materials and substrates also plays a key role in flexible devices. Various substrates are available, which can be used in flexible devices such as PET (Polyethylene Terephthalate), PDMS (polydimethylsiloxane), Polyester, Kapton, etc. [204]. Organic semiconductor materials with high molecular weight have various advantages in terms of processing at low-temperature, self-assembly, good solubility in organic solvents, etc. [205]. The selection of suitable dielectric material, semiconductor, and processing method have very important roles in fabricating high-performance flexible OTFT device.

Recently various flexible OTFT device has been explored using polymer dielectrics such as polyacrylic acid (PAA)/ poly(methyl methacrylate) (PMMA) [182], P(VDF-TrFE)/ PMMA [206], PVA/HfO_2 [207], etc. due to their low-temperature processing, high solubility, bendable ability and compatibility with organic semiconductors. The problem with polymer dielectrics is they generally have a low dielectric constant; thereby, it is somewhat challenging to fabricate a low-voltage flexible device with these polymer-based dielectrics [208]. The device operated at high voltage suffers from large dynamic power dissipation ($P_d \propto V_{DD}^2$), which is inappropriate for high-performance and reliable OTFTs [209]. The areal capacitance

of the dielectric film can be enhanced by either reducing the thickness of the dielectric film [208] or by choosing a material with a high-k value [210]. As a gate oxide, the high-k dielectric material can suppress these problems as it passes with a high dielectric constant [160]. Although the high-k dielectric inorganic oxide has several advantages in terms of low cost, minimal wastage, simple fabrication steps, large area fabrication, etc., but the synthesis of thin, smooth, uniform, and low-temperature processed inorganic oxide dielectrics are quite complex. Moreover, the problem with the solution-processed pristine inorganic oxide dielectric layers is that they are usually brittle in nature and require high-temperature processing, so the pristine inorganic oxide materials are not suitable for flexible electronics [211]. These problems can be overcome by suitable UV-assisted synthesized hybrid dielectric materials (Inorganic oxide polymer nanocomposite) as a gate oxide layer [211].

In the present work, low-temperature processed hybrid dielectric (ZrOx/PMMA/Poly melamine co-formaldehyde (PMCF)) as a gate oxide and P3HT/ (graphitic carbon nitride) g-C_3N_4 nanocomposite as an active semiconductor material has been utilized to fabricate an efficient, flexible OTFT sensor for ammonia gas at RT-25 ºC. The introduction of 2D nanomaterials in the pristine polymer enhances the crystalline and electrical characteristics and also improves the sensitivity for the NH_3 analyte [16].

Recently, ammonia gas sensors have gained considerable interest due to their numerous applications in industries such as in refining, manufacturing plants, nitrogenous fertilizers, and refrigeration [17]. Detecting this toxic analyte has a great interest in the industry and environmental monitoring, as prolonged exposure to NH_3 can damage living organisms' eyes, skin, and respiratory systems [16] [17]. Recent progress on ammonia sensors includes Metal

oxide sensors WO_3 [200], Pt-Ge_2O_3 [212], etc., which requires high temperature for operation and sensors based on conjugative polymer-nanocomposite-based sensing film, such as P3HT/rGO [213], PQT-12/CdSe [196], PBTTT [17], etc., etc. These conjugative polymers based TFTs utilize SiO_2 for the gate oxide layer require high voltage for operation, not suitable for low power and flexible electronic applications. A handful of solution-processed TFT articles are also available for ammonia sensor operated at low voltage operation including [177](dielectric-Li_5AlO_4), [214](dielectric- P(VDF-TrFE-CFE); however, the fabrication process have been done on rigid silicon/glass substrate. Due to these reasons, the authors motivate to find an efficient, reliable, low-voltage, cost-efficient, flexible OTFT-based ammonia sensor at RT operation. The motive of this extensive study is to find a low-power, solution-casted, cost-effective, flexible organic TFT for ammonia sensors and other portable electronic (flexible memories, flexible LEDs), sensing (pH sensors, biosensors), and medical applications in nearby future.

5.2 Experimental Procedure

5.2.1. Chemical Procured

P3HT (Poly(3-hexylthiophene-2,5-diyl) (MW 50k -75k) was procured from Sigma Aldrich Pvt. Ltd. All the other chemicals were procured from Merck India pvt. Ltd. and used as it is without any further purifications.

5.2.2. Device Fabrication Steps

The device fabrication process is as follows-

An Indium tin oxide-coated Polyethylene terephthalate substrate (ITO/PET) (15 mm×20 mm) was thoroughly cleaned with acetone and propanol for 10 minutes each. Subsequently, the ITO-coated PET substrate was rinsed by running DI water. After that, the cleaned

substrate was put under N_2 ambient in a hot oven at 80 °C temperature for 50 minutes to eliminate the DI water droplets from the cleaned surface. The dried substrate was then put on an oxygen plasma treatment for 20 min. to form a cleaned, hydrophilic, adhesive substrate surface with uniform surface energy.

A 100 mM of ZrAc powder and 50 mg/ml of PMMA crystal were dissolved separately in 2ME solvent for a ZrAc and PMMA homogenous solution. The ZrAc, PMMA, and PMCF solution were mixed in 1 M: 0.15 M: 0.20 M ratio and stirred over 900 rpm at 60 ºC for 12 hours to form a homogenous ZrAc/PMMA/PMCF hybrid dielectric solution. The molar concentration of the hybrid solution has been optimized for smooth film spreading, high dielectric areal capacitance, and low surface roughness for spin coating. After that, a 0.22 μm PTFE syringe filter was used to filter the hybrid dielectric solution to eliminate large/heavy size particles. The hybrid dielectric solution was then spin-coated on a cleaned plasma-treated ITO/PET substrate at 3000 rpm for 60 seconds to get a uniform synthesized film. The spin-coated film was further annealed in a hot oven at 100 °C for 24 hours to eliminate the organic solvent residues. Afterward, the synthesized layer was exposed to a medium-pressure metal halide UV lamp of 55 mW/cm^2 power intensity for 60 minutes to form a 55±4 nm (Measured by Filmetrics F20-UV) dielectric film. Further, the dielectric film was exposed to a vapor phase HMDS (Hexamethyldisilazane) treatment to form a hydrophobic self-assembled monolayer.

A UV photoirradiated (275 nm for 10 min.) 10 mg/ml P3HT in $CHCl_3$ solution, mixed with g-C_3N_4 2D material to form a 5% wt/wt polymer nanocomposite solution, was utilized for floating film transfer (FTM) deposited organic semiconductor film. A brief idea about the

FTM process is illustrated in **Figure 1.5**.

The thermal coating unit HHV 12A4D was used to deposit a 70 nm thick (@ 0.1 Å/sec.), 50 µm length and 18.03 mm width gold source/drain contact at a pressure of 10^{-6} torr. The device schematic and image are given below in **Figure 5.1(a)** and **Figure 5.1(b),** respectively.

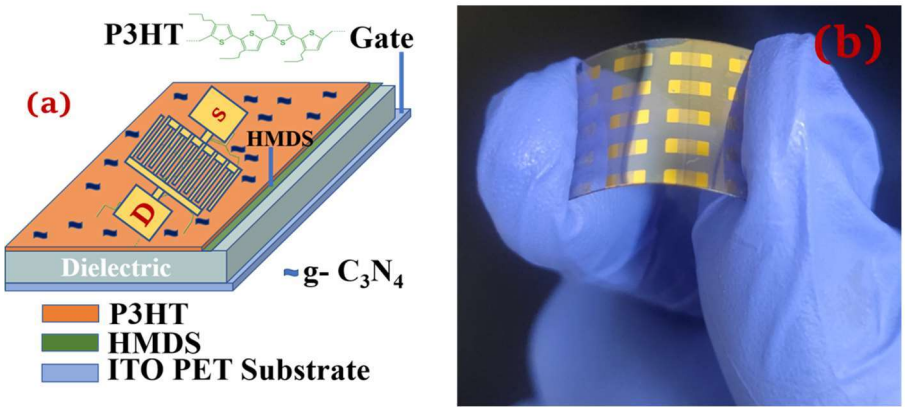

Figure 5.1 (a) Geometry, (b) Image of fabricated flexible organic TFT.

5.3 Thin Film Characterization and Sensing Setup

5.3.1. Thin Film Characterization

The XRD peaks of P3HT/g-C_3N_4 in **Figure 5.2(a)** at 6.07º, 11.7º, 16.18º, and 26.7º are responsible for (100), (200), (300), and (002) planes, respectively[16][215]. The plane at (002) in the polymer nanocomposite matrix validates the trace amount of g-C_3N_4 2D nanomaterial in the pristine P3HT polymer matrix. The XRD peaks of ZrOx at 28.68º, 30.78º, and 38.1º are responsible for (111), (200), and (120) planes, respectively. The XRD pattern of the ZrOx/PMMA/PMCF hybrid dielectric has an additional broad peak to ZrOx at 14.5º, which validates the PMMA in the inorganic ZrOx.

The capacitance per unit area of the hybrid dielectric/oxide film was measured by the semiconductor parameter analyzer's Capacitance vs. Frequency sweep shown in **Figure 5.2(b)**. The hybrid dielectric (ZrOx/PMMA/PMCF) film exhibited a good areal capacitance of 310

nF/cm^2 (k value ~20 at 55 nm thickness) at -2 V, creating a high charge in the semiconductor channel, which reduces the operating voltage of the OTFT device. In addition to high areal capacitance, the photon energy (hv) vs. sqr (αhv) or tauc plot of the dielectric film in **Figure 5.2(c)** exhibited the band gap of the ZrOx/PMMA/PMCF film is 5.27 eV., which is sufficient enough to use the synthesized dielectric as a gate oxide layer. The hybrid dielectric's current density plot in **Figure 5.2(d)** offers a very low leakage current density (~10^{-9} A/cm^2 at -2 V gate voltage), which shows the dielectric film is almost free from pin holes.

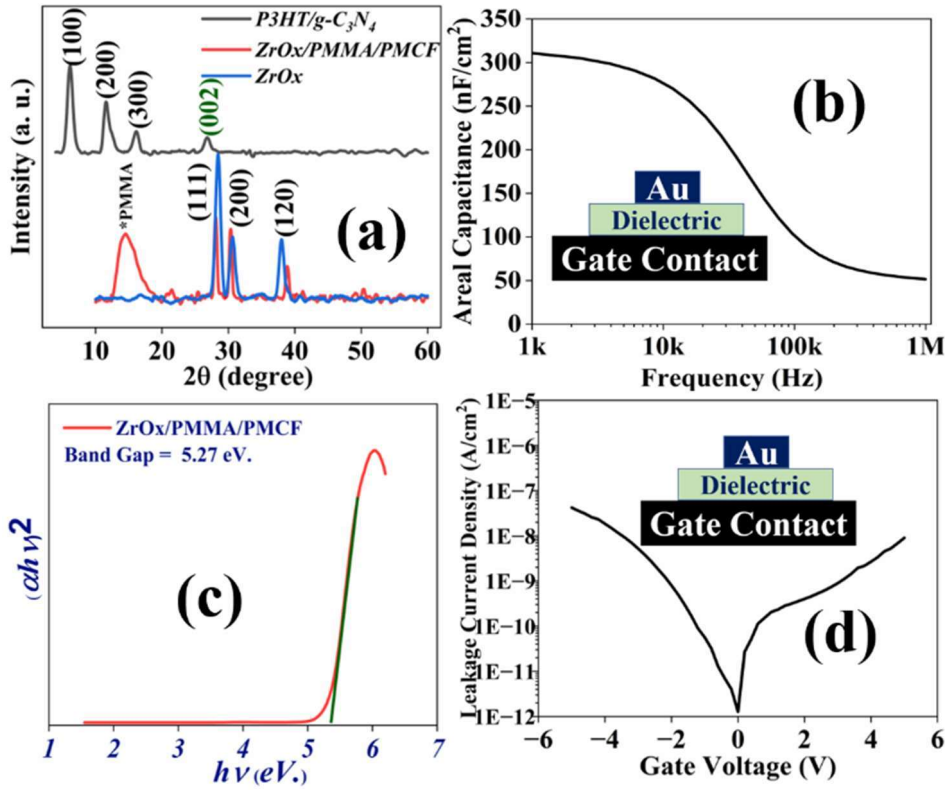

Figure 5.2 (a) XRD pattern of P3HT/g-C_3N_4, ZrO_x/PMMA/PMCF hybrid dielectric, ZrOx dielectric films, (b) Capacitance vs. frequency plot, (c) Band gap (Tauc plot), (d) Leakage current density plot, of the hybrid dielectric film.

The morphology of the spin-coated hybrid dielectric film over ITO/PET, shown in **Figure 5.3(a)**, illustrates that the surface of the hybrid dielectric film is quite smooth (avg. RMS

roughness 0.388 nm) and favorable for OTFT fabrication. The AFM morphology of FTM transferred polymer film offers active sites for adsorption and desorption sites for gas molecules, which is shown in **Figure 5.3(b)**. The surface roughness (1.413 nm) of the polymer nanocomposite film offers a large no. of adsorption/desorption sites, which is advantageous for gas sensing performance.

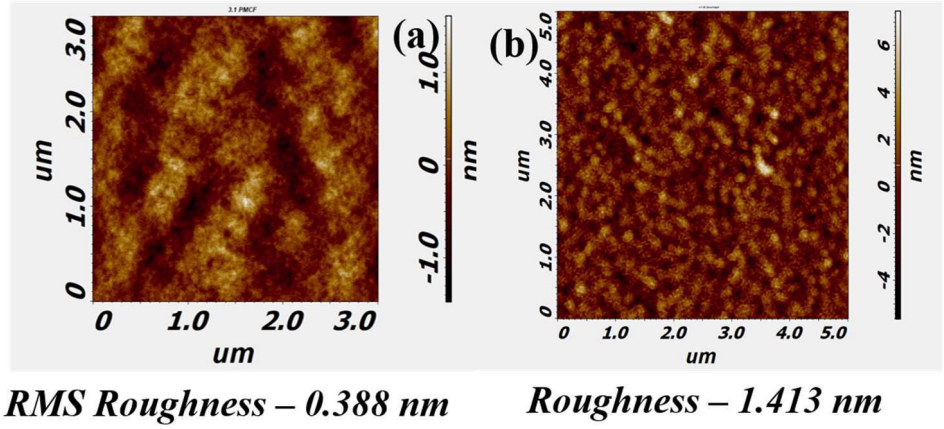

Figure 5.3 Atomic force morphology of (a) Synthesized ZrO_x/PMMA/PMCF dielectric film, (b) FTM deposited organic polymer nanocomposite film.

5.3.2. Sensing Setup

Our customized sensing setup, with a mass flow controller connected by a sample gas cylinder, has been used for all sensing measurements. The chamber also has a humidity sensor, mixing fan, and probe setup connected to the semiconductor device analyzer model Agilent B1500A for various sensing characterizations. All the sensing measurements have been done at room temperature in the ambient air and ~55% relative humidity. A schematic of the sensing setup is shown in **Figure 3.5**.

5.4 Device Characteristics and Sensing Results

In the current section, the various I/V characterization of the device and sensing mechanism

has been briefly explained.

5.4.1. Drain Characteristics

The drain characteristics of the device have been plotted in **Figure 5.4(a)** shows that the device has the ability to operate at a low voltage of -2 V with a good saturated drain current of -2.0 µA.

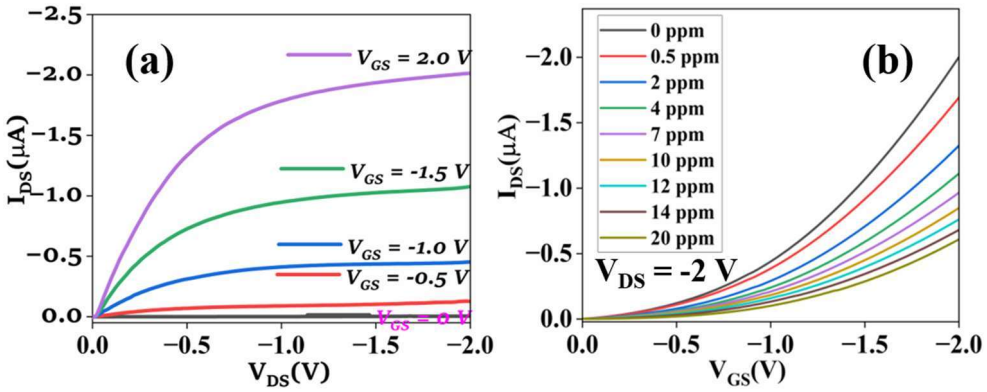

Figure 5.4 (a) Drain curve characteristics (I_{DS}-V_{DS}) plot of the fabricated flexible OTFT sensor, (b) Transfer curve (I_{DS}-V_{GS}) curve with exposed ammonia analyte (0-20 ppm).

The high-k ZrOx/PMMA/PMCF material as a gate oxide offers high charge density or enhances the areal capacitance, resulting in low voltage operation of the flexible OTFT. The drain current of the organic TFT in saturation regime can be expressed as-.

$$I_{DS}^{sat} = \frac{W}{2L}\mu_p C_{OX}(V_{GS} - V_{TH})^2 \; ; \; V_{DS} \geq V_{GS} - V_{TH} \tag{5.1}$$

5.4.2. Bending or Flexibility Test

In order to investigate the bending/rollable test, the transfer characteristics of the device have been characterized by the curved holder shown in **Figure 5.5(a)**. The transfer curve of the device characterized by a curved holder with bending radii of flat, 20 mm, 15 mm, 10 mm, and 5 mm have been plotted in **Figure 5.5(b)**. It has been observed that the fabricated flexible device can withstand upto a bending radius of 10 mm efficiently. Below the 10 nm bending

radius, the device undergoes deform characteristics shown in **Figure 5.5(b)** for a 5 mm bending radius, but when the bending stress is removed, the device regains its original characteristics. In other words, no permanent degradation in the electrical performance of the device has been found upon the removal of bending strain.

Table 5.1 shows the relative change in the device parameters with the applied bending test. A negligible change in the device parameters in **Table 5.1** is probably due to a very minute degradation in the charge transport phenomenon of the flexible TFT. The enhanced flexible performance of the device is due to PMMA/PMCF in the ZrOx dielectric solution.

Table 5.1 Extracted Parameters with a Bending Radius

Parameters	Flat	20 mm	15 mm	10 mm
V_{TH}	-0.1052	-0.1120	-0.1246	-0.1308
μ_p (cm^2/V.Sec.)	0.1073	0.1025	0.09346	0.09385
I_{DS} (μA)	2.00337	1.94541	1.8746	1.79938

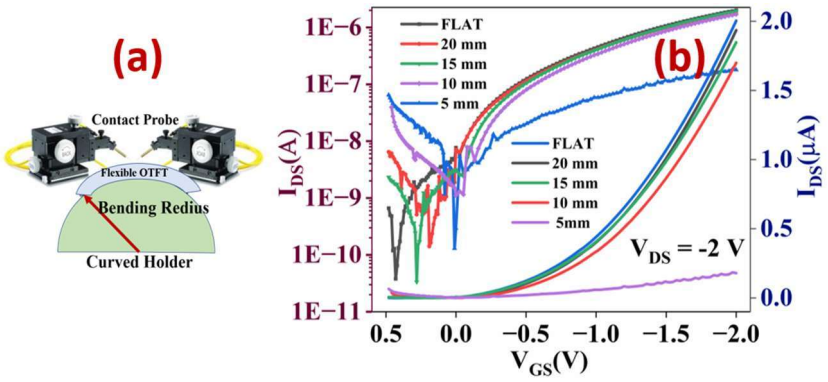

Figure 5.5 (a) Bending test setup schematic, (b) Transfer curve characteristics of the device with different bending radius of substrate.

5.4.3. Sensing Results

5.4.3.1. Sensing Response

The sensing results of the fabricated flexible ammonia sensor have been characterized by the

transfer characteristic of the device at -2V V_{DS} supply. The transfer characteristic, shown in **Figure 5.4(b)**, has been utilized for sensing characterization due to its multiparameter characteristic in terms of threshold voltage (V_{TH}), mobility (μ_p), subthreshold swing (SS), etc. The sensing response of the flexible ammonia sensor can be defined as [16]

$$S\% = \left|\frac{I_{DS\,(air)} - I_{DS(NH_3}}{I_{DS(air)}}\right| * 100 \quad (5.2)$$

Where $I_{DS\,(air)}$ and $I_{DS(NH3)}$ represent the drain current in ambient air and over the exposed ammonia analyte, respectively.

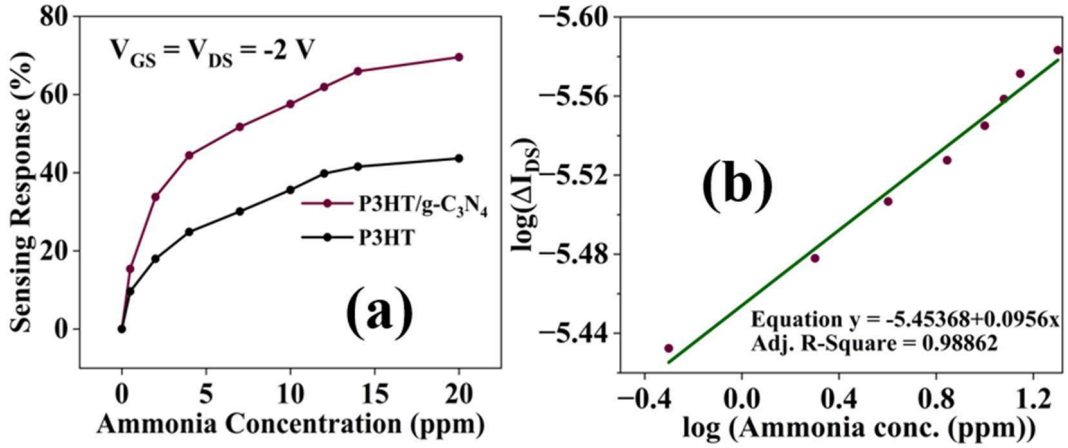

Figure 5.6 (a) Gas sensing Response with exposed NH_3 gas, (b) Logarithmic plot of change in I_{DS} for various log concentrations of NH_3.

In the present work, the gas sensing response characteristics of P3HT and P3HT/g-C_3N_4 are plotted in **Figure 5.6(a)** over a range of 0 to 20 ppm ammonia gas. The introduction of g-C_3N_4 material in the P3HT matrix enhances the sensing response of the fabricated sensor. The sensing response plot in **Figure 5.6(b)** has a good linear response over the lower concentration range and is saturated with high ppm ammonia gas. The saturation phenomenon is due to fewer no. of available active sites for the gas molecules at higher NH_3 concentrations. The logarithmic change in the drain current with log ammonia gas concentration plot

in **Figure 5.6(b)** shows that the curve has a good correlation coefficient of 0.988 over 0 to 20 ppm NH_3 concentration.

5.4.3.2. Device Parameters with Exposed Ammonia Gas

The various device parameters to analyze the effect of the exposed analyte over the sensing surface of the flexible sensor have been characterized by the transfer characteristics of the device shown in **Figure 5.4(b)**. The V_{TH}, μ_p, and SS calculations are given by equations (5.4) and (5.5), respectively. From equation (5.1)-

$$\sqrt{I_{DS}^{sat}} = \sqrt{\frac{1}{2}\mu_p C_{OX}\frac{W}{L}}\,(V_{GS} - V_{TH}) = XV_{GS} - Y \tag{5.3}$$

The V_{TH} and μ_p of the transistor are calculated graphically by a linear equation in –

$$\mu_p = \frac{2L}{WC_{ox}}X^2 \quad \& \quad V_{TH} = \frac{-Y}{X} \tag{5.4}$$

The subthreshold swing (SS) and trap charge density of the transistor are calculated by-

$$SS = \frac{dV_{Gs}}{d(log(I_{Ds}))} \quad \& \quad \Delta_{Trap} = \frac{\Delta V_{TH} * C_{OX}}{q} \tag{5.5}$$

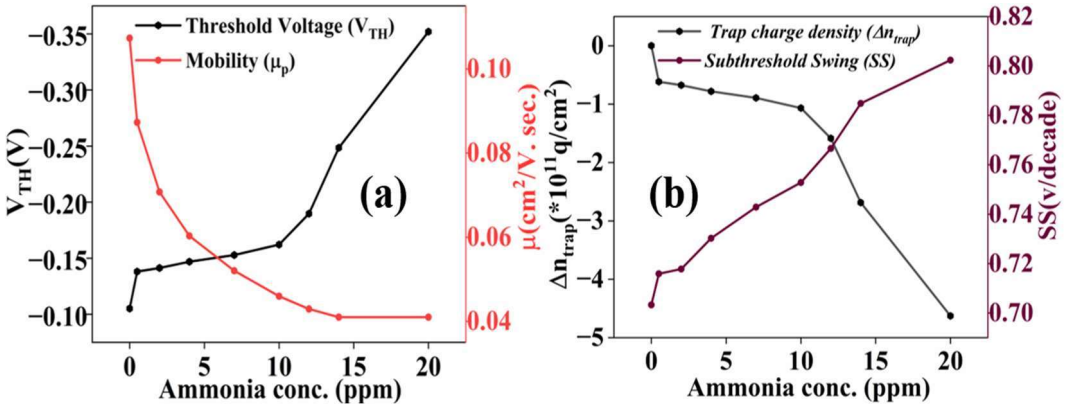

Figure 5.7 (a) Change in the V_{TH} and μ_p with varying NH_3 gas, (b) Trap charge density and SS variation with the exposed ammonia analyte.

The graphs in **Figure 5.7(a)** and **Figure 5.7(b)** show V_{TH} and *SS* increases while the μ_p decreases with the NH_3 gas concentration due to the I_{DS} decreasing with exposed NH_3 gas.

The NH_3 gas molecules trap the active charge carriers at the sensing surface and deplete the number of charge carriers in the channel, thereby reducing the I_{DS} of the fabricated flexible OTFT. **Table 5.2** illustrates various parameters with exposed NH_3 gas.

Table 5.2 Extracted Parameters with Exposed NH_3 Gas

NH_3 gas (ppm)	V_{TH} (V)	μ_p (cm^2/V. sec.)	Δn_{trap} (C/cm^2)	SS (V./decade)	S (%)
0	-0.1052	0.1073	0	0.717	0
0.5	-0.1381	0.0873	6.16E10	0.703	15.39616
2	-0.1413	0.0707	6.77E10	0.715	33.77055
4	-0.1469	0.0603	7.81E10	0.730	44.41993
7	-0.1529	0.0520	8.94E10	0.742	51.71799
10	-0.1522	0.0459	8.81E10	0.752	57.55829
12	-0.1898	0.0429	1.58E11	0.766	61.92236
14	-0.2485	0.041	2.68E11	0.784	65.94586
20	-0.3520	0.041	4.62E11	0.802	69.55876

5.4.3.3. Effect of Relative Humidity on the Sensing Response

The effect of the relative humidity (RH) is an important factor that must be analyzed for a reliable sensor. The plotted I_{DS} vs. Time graph with 20 ppm ammonia gas in **Figure 5.8(a)** shows that the sensing response is almost independent of the RH factor over a range of 20 to 70%. A little drop in the number of reactive sites in the sensing channel caused by water molecules is likely the cause of the minimal change of 6%-7% in the sensing response that has been recorded over an RH range of 20%-70%. A minute no of water molecules adsorbed over the active sites decreases the available active sites for gas adsorption; hence a minute drop in the sensing response has been seen with RH variation [149].

5.4.3.4. Selectivity Investigation of the Fabricated Sensor

To test the selectivity of the manufactured device, the selectivity of the sensor for a variety of common interfering gases, including H_2S, CH_4, CO, CO_2, H_2, and LPG, has been

examined. The manufactured flexible sensor is highly selective for NH_3 gas, as shown by the selective bar chart in **Figure 5.8(b)**.

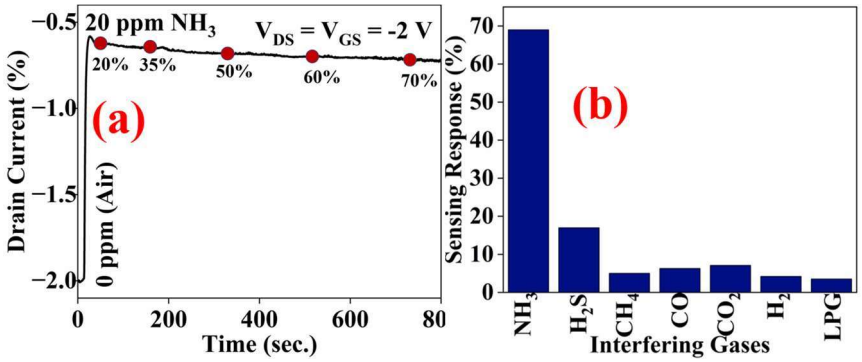

Figure 5.8 (a) I_{DS} vs. Time plot with varying relative humidity over 20 ppm ammonia gas, (b) Selectivity of the fabricated sensor for common interfering gases (NH_3, H_2S -20 ppm, CH_4, CO, CO_2, H_2, LPG- 50 ppm).

5.4.3.5. Transient Response and Stability

The fabricated device underwent a transient investigation to examine the sensor's response/recovery time, and repeatability for the NH_3 analyte. The response time of the OTFT sensor is defined as the time taken by the sensor to reach 90% of the final drain current after the exposed analyte. In contrast, recovery time can be given by the time required for the gas sensor to return 90% of the final baseline after the target gas has been removed. The transient response/repetitive response of the fabricated sensor toward the NH_3 analyte has been illustrated in **Figure 5.9(a)**. The Response ($T_{res.}$), and the Recovery Time ($T_{rec.}$) of the sensor are 4±0.5 sec. and 36±4 sec, respectively. The sensor also follows a good degree of repetitive response towards the NH_3 gas at RT operation.

The sensing response stability of the fabricated sensor has been recorded over 23 days at 20 ppm NH_3 gas. The sensor's response in **Figure 5.9(b)** shows that the sensor is almost stable (6% relative deviation) over 23 days. The introduction of g-C_3N_4 in P3HT and annealing temperature for the dielectric film and polymer nanocomposite film has great importance in

enhancing the stability of the sensor for a long time. The introduction of g-C_3N_4 in the P3HT matrix suppresses moisture absorption and improves the relative stability of the polymer nanocomposite film.

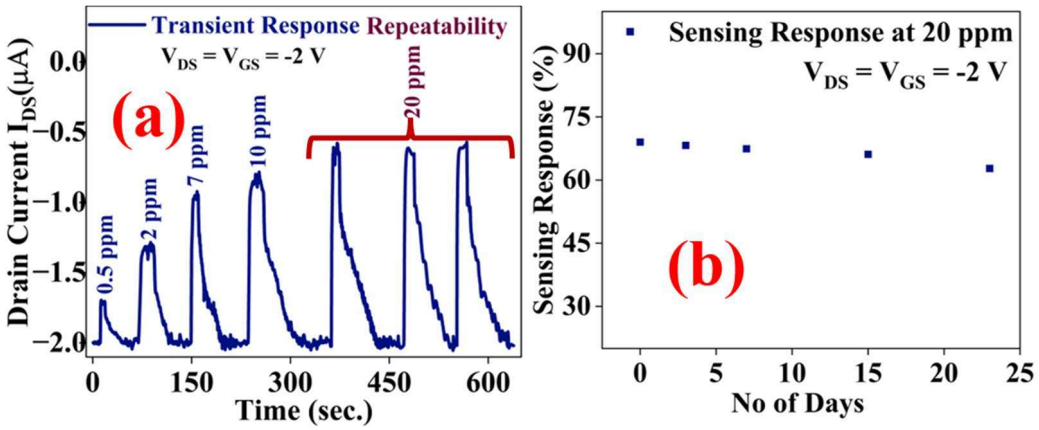

Figure 5.9 (a) Transient response with exposed ammonia concentration, (b) Stability in the sensing response over 23 days.

5.4.4. Qualitative/Comparative Test

The qualitative study is important to check and compare the fabricated device's performance for the ammonia analyte. **Table 5.3** demonstrates the qualitative/comparative test of the fabricated ammonia sensor.

Table 5.3 Comparative Study of the Fabricated Gas Sensor

Sensor Type	Sensing Material	S% (ppm)	O.V. (V)	$T_{res.}$ /$T_{rec.}$ (sec.)	Remark [Ref.]
MO	WO_3	40(5 ppm)	2	23/25	High temp. operation (250 ºC) [200]
MO	Pt-Ge_2O_3	3.2(1 ppm)	2	214/107	Poor response time/ Response, high operating temperature [212]
Optical	PbSe	-	3	>60	Complex and costly setup [216]
Chemi.	CuO/Ws_2	60(60 ppm)	-	35/213	Poor sensing response and recovery time [217]
Chemi.	rGO/$MoSe_2$	0.563(3 ppm)	-	14/19	Poor response time [218]
OTFT	PBTTT	89(100 ppm)	-60	26/44	Low response, high operating voltage [17]
OTFT	P3HT/MoS_2	63(80 ppm)	-60	-	Low response, high operating voltage [16]
OTFT	PQT-12/CdSe	51(100 ppm)	-40	65/240	Low sensing response and high operating voltage[196]
OTFT	DPPT-TT	10 (2 ppm)	-3	-/30 min	Very poor recovery time, poor response [214]
OTFT	P3HT/g-C_3N_4	69(20 ppm)	-2	4/38	Low operating voltage, high response, flexible TFT [This Work]

MO – Metal Oxide, Chemi. – Chemiresistive, O.V. – Operating Voltage, Tres. /$T_{rec.}$ -Response/Recovery time, S% (conc.) – Sensing response (concentration of ammonia)

5.4.5. Device Physics and Sensing Mechanism

The current section is divided into two parts- (a) Fabricated device mechanism and (b) Gas sensing mechanism. The fabricated device passes with enough saturation current, as shown in **Figure 5.4(a)**, due to the high areal capacitance (310 nF/cm^2, k value ~ 20 at 55 nm thickness) of the ZrOx/PMMA/PMCF material as a gate oxide layer. The high areal capacitance of the hybrid dielectric layer generates enough charge accumulation in the semiconductor channel at a lower voltage, which is responsible for the low voltage operation of OTFT [219]. In addition, the hybrid dielectric layer as a gate oxide improves the flexibility strength compared to the pristine inorganic oxide dielectric ZrOx; as most of the pristine inorganic oxide, dielectric films are brittle in nature [220]. The polymer material PMMA/PMCF in ZrOx dielectric improves the flexible strength of the gate oxide layer, which is probably due to the epoxy nature of PMMA/PMCF material. The PMCF also works as a binder/crosslinking agent for the ZrOx and PMMA dielectric layer, thereby improving the flexible strength and also smoothness of the gate oxide layer (refer to AFM **Figure 5.3**(a)). The smoothness of the gate oxide layer further improves the mobility of the flexible TFT due to suppressed scattering phenomenon with a smoother surface [221]. Moreover, the FTM deposited, UV photoirradiated polymer nanocomposite film over the hybrid dielectric layer doesn't damage the gate oxide layer because FTM didn't use any rotational (Spin Casting) or drag (Blade coating, Langmuir Blodgett, etc.) mechanism, resulting in an enhanced quality organic semiconductor film growth. The UV photoirradiated polymer nanocomposite solution became photoexcited, resulting in improved self-assembly and ordered molecular chain of the solution, which can

be seen in the XRD pattern of the polymer nanocomposite film [16][222]. The photoexcited polymer nanocomposite solution results in an enhanced π orbital overlapping along the polymer's backbone and subsequent chain planarization, allowing an enhanced delocalization of π electrons. The planarized polymer chain begins to interact with the 2D g-C_3N_4 through many nucleation growth sites, which is favorable for nucleation growth with fewer defects and vacancies and forms better π-π interaction on the nucleation sites [178][222].

Table 5.4 Extracted Parameters from the CV Plot in Figure 5.10(b)

Energy Level	P3HT/g-C_3N_4 before NH_3 Exposed	P3HT/g-C_3N_4 After NH_3 Exposed
E_{ox} (Onset)	0.80 V	0.81 V
E_{red} (Onset)	-1.10 V	-1.26 V
HOMO	-5.20 eV.	-5.21 eV.
LUMO	-3.31 eV.	-3.15 eV.
Band gap	1.89 eV.	2.06 eV.

E_{HOMO} = -(4.4+E_{ox} (onset)) eV. [178]., E_{HOMO}-E_{LUMO} = Band Gap

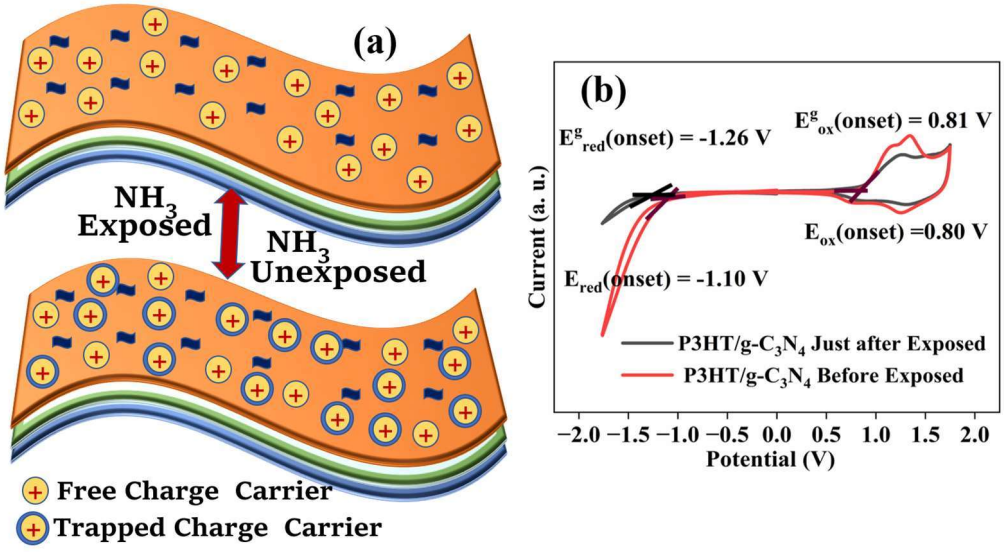

Figure 5.10 (a) Doping/de-doping mechanism at the sensing surface, (b) CV plot of polymer nanocomposite film before and after NH_3 exposure.

In the gas sensing mechanism incorporating the 2D g-C_3N_4 in the pristine P3HT polymer enhanced the crystalline property and chain ordering due to enhanced π-π electron coupling,

which improves the polaron delocalization over the sensing surface, enhancing the charge transport and fast sensing of the device. The sensing mechanism can be better understood with the help of **Figure 5.10(a)**. The sensing mechanism for ammonia gas at the P3HT/2D g-C_3N_4 surface can be described by the carrier doping/de-doping phenomenon. The conductivity of the active/sensing film of organic TFT was changed when the exposed ammonia interacted with the sensing surface. The ammonia gas, as a donor or extrinsic defects, donates its lone pair of electrons to the sensing surface; the electrons will trap the active charge carriers or deplete the active charge carriers, i.e., holes in the p-channel TFT, modulating the drain current, threshold voltage, mobility of the flexible OTFT sensor [16][167]. The interaction process can be further validated by the Cyclic Voltammogram (CV) plot in **Figure 5.10(b)**. The interaction of ammonia gas molecules over the polymer/2D nanocomposite sensing surface creates an additional lowest unoccupied molecular orbital (LUMO) level, which increases the material's band gap and reduces the drain current of the organic TFT. A Cyclic Voltammogram plot in **Figure 5.10(b)** validates the creation of an additional LUMO level and an enlarged band gap of the sensing polymer/2D nanocomposite surface from 1.89 eV. to 2.06 eV. upon exposure to ammonia gas. **Table 5.4** shows the changes in the energy level of the P3HT/g-C_3N_4 nanocomposite with exposed ammonia gas. A sensor's response/recovery time for any target gas will depend upon the sensing surface's adsorption (surface property) or diffusion (bulk property) phenomenon. Moreover, the introduction of g-C_3N_4 nanosheets in polymer matrix processes a 2D nanostructure and Vander wall interaction in the presence of-NH_2 or-NH (NH_3 gas in this work) and form a physisorption of ammonia gas molecules over the surface of polymer/2D g-C_3N_4 matrix via weak Vander Waals or electrostatic interactions, which enhance the sensing response and improves the transient response

(response/recovery) time for the fabricated sensor. In the present work, the optimized thickness of the sensing film follows a dominant adsorption process over diffusion, which results in a speedy sensing response. Another possible reason for the fast response and recovery time is probably due to weak van der wall forces between the ammonia molecule and P3HT/g-C_3N_4 nanocomposite film.

5.5 Conclusion and Future Scope

A flexible low-voltage operated TFT has been developed and utilized for the ammonia gas sensor at RT operation. The fabricated device utilizes a low-temperature UV-cured solution-processed hybrid dielectric layer, which offers a high area capacitance of 310 nF/cm^2 (k ~20), low leakage current density of ~10^{-9} A/cm^2 at -2 V, and a high band gap of 5.27 eV. A 35±4 nm polymer/2D nanocomposite film has been deposited by a cost-effective floating film transfer technique to synthesize a uniform thin active layer. The device offers a low threshold voltage of -0.1052 V with improved mobility of 0.1073 cm^2/V. sec., can be further utilized in low-power portable electronic and sensing applications. The device has the advantages of both the hybrid dielectric polymer in terms of flexible, low voltage operation (-2 V) and FTM deposited active film in terms of self-assembly, simple, and cost-efficient technique. The bending test of the device also shows good mechanical flexibility of the fabricated flexible sensor. The fabricated organic TFT for ammonia sensing has a low detection of 500 ppb and a sensing response of 69% at a 20 ppm analyte. Additionally, the fabricated flexible sensor also offers a fast response/recovery time of 4±0.5/36±4 sec, respectively. The present study aims to fabricate a low-cost, solution-casted, low-voltage, flexible organic TFT utilizing a hybrid inorganic/polymer dielectric layer for various electronic (flexible memories, flexible LEDs), sensing (pH sensors, biosensors) and medical applications.